Plant Physiology and Biochemistry 143 (2019) 142–153

Contents lists available at ScienceDirect

Plant Physiology and Biochemistry

journal homepage: www.elsevier.com/locate/plaphy

Research article

Physiological and iTRAQ based proteomics analyses reveal the mechanism of elevated CO_2 concentration alleviating drought stress in cucumber (*Cucumis sativus* L.) seedlings

Qingqing Cui[a,c,1], Yiman Li[a,1], Xinrui He[a], Shuhao Li[a], Xin Zhong[a], Binbin Liu[b], Dalong Zhang[a,b,*], Qingming Li[a,b,**]

[a] College of Horticulture Science and Engineering, Shandong Agricultural University, Tai'an, 271018, China
[b] State Key Laboratory of Crop Biology, Tai'an, 271018, China
[c] Institute of Vegetables and Flowers, Chinese Academy of Agricultural Sciences, Bei'jing, 100081, China

ARTICLE INFO

Keywords:
Cucumber seedling
Chloroplast
Elevated [CO_2]
Drought stress
Proteomics analyses
iTRAQ

ABSTRACT

Carbon dioxide is one of the most important anthropogenic greenhouse gases. We previously confirmed that elevated [CO_2] alleviated the negative consequences of drought stress to cucumber seedlings, but the physiological mechanism remains unknown. We investigated the morphological and physiological characteristics as well as iTRAQ-based proteomics analyses in this study under different combinations [CO_2] (400 and (800 ± 20) μmol·mol^{-1}) and water conditions (no, moderate and severe drought stress simulated by polyethylene glycol 6000). The results showed: (1) elevated [CO_2] significantly increased plant height, stem diameter, leaf area and relative water content (RWC) under drought stress; (2) drought stress significantly increased J and K peaks of the chlorophyll *a* fluorescence transient, indicating the damage of photosynthetic electron transport chain, while elevated [CO_2] decreased them especially under moderate drought condition; (3) iTRAQ-based proteomics analyses indicated that elevated [CO_2] increased the abundance of psbJ and the PSI reaction center subunit VI-2 in seedlings exposed to moderate drought stress; (4) the abundance of uroporphyrinogen decarboxylase 2 and tetrapyrrole-binding protein decreased in response to elevated [CO_2] under severe drought condition; (5) elevated [CO_2] regulated the expression of chloroplast proteins such as those related to stress and defense response, redox homeostasis, metabolic pathways. In conclusion, elevated [CO_2] enhanced the efficiency of photosynthetic electron transport, limited the absorption of excess light energy, enhanced the ability of antioxidant and osmotic adjustment, and alleviated the accumulation of toxic substances under drought stress. These findings provide new clues for understanding the molecular basis of elevated [CO_2] alleviated plant drought stress.

1. Introduction

Global climate change is driven by an increasing atmospheric CO_2 concentration (A[CO_2]), which leads to temperature extremes and alters precipitation patterns, impacting plant growth and productivity (Feng et al., 2014). The A[CO_2] is predicted to increase from current levels of approximately 400 μmol mol^{-1} to 730–1020 μmol mol^{-1} by the end of the century (Canadell et al., 2007; Bala, 2013). Elevated CO_2 concentration (E[CO_2]) reportedly promoted drought tolerance or mitigated damages due to drought stress in various plant species, especially C_3 species (Kirkham, 2011). E[CO_2] increased photosynthetic rates, reduced stomatal conductance, induced rapid stomatal closure, which can lead to reducing plant water loss (Ainsworth and Rogers, 2007; Hsu et al., 2018). Photosynthesis is one of the most important processes in plants (Baker, 1991), negative effects of drought stress on its performance will decrease crop productivity (Carmo-Silva et al., 2012; Ghotbi-Ravandi et al., 2014). The chlorophyll *a* fluorescence signal can be used as a probe for photosynthetic activity, and to monitor regulatory processes affecting the PSII antenna (Kalaji et al., 2016). The chlorophyll *a* fluorescence transient measured under high light shows a typical O-J-I-P polyphasic rise (Strasser, 1997). Chloroplast as a site for photosynthesis conducts many complex biochemical and biophysical processes, the operation of chloroplasts depends on the assembly and homeostasis of thousands of proteins, and chloroplast proteins are

* Corresponding author. College of Horticulture Science and Engineering, Shandong Agricultural University, Tai'an, 271018, China.
** Corresponding author. College of Horticulture Science and Engineering, Shandong Agricultural University, Tai'an, 271018, China.
E-mail addresses: zdl0531@126.com (D. Zhang), gslqm@sdau.edu.cn (Q. Li).
[1] These authors contributed equally to this work.

https://doi.org/10.1016/j.plaphy.2019.08.025
Received 11 July 2019; Received in revised form 26 August 2019; Accepted 27 August 2019
Available online 29 August 2019

subject to proteolytic regulation, which plays important roles in maintaining normal organellar functions and in delivering responses to developmental and environmental cues (Ling et al., 2019). There is little information on the effects of E[CO_2] or drought stress on chloroplast proteins (Kosmala et al., 2012), even less is known about the interactive effects of these environmental variables on chloroplast proteins.

Cucumber (*Cucumis sativus* L.) is one of the most popular greenhouse-grown vegetables worldwide, and is the predominant vegetable grown in solar greenhouses in northern China. We previously confirmed that E[CO_2] increased photochemical efficiency, apparent quantum efficiency and maximum CO_2 assimilation rate of cucumber seedlings under moderate drought conditions (Li et al., 2008, 2011), and improved the antioxidant capacity by accumulating L-gulonolactone, pyrocatechol and 1,2,3-trihydroxybenzene, and improves osmotic adjustment by accumulating glutamate of cucumber seedlings under severe drought conditions (Li et al., 2018), which ultimately alleviated or offset the negative consequences of drought stresses. However, chloroplast protein profiles of cucumber plants in response to CO_2 enrichment and drought stress have not been clearly investigated. Isobaric tags for relative and absolute quantitation (iTRAQ) based proteome analysis have been carried out to elucidate mechanisms of abiotic stress responses in plant species such as maize (Benešová et al., 2012), grape (Liu et al., 2014), because of its higher identification rate of low abundance proteins and more accurate quantification of proteins as compared to traditional 2D gel electrophoresis analysis (Zieske, 2006). Therefore, the aim of this study is to elaborate the mechanism of E[CO_2] alleviating drought stress by the iTRAQ based proteome analyses of chloroplast of cucumber seedlings, which also may provide a theoretical basis for CO_2 fertilization for cucumber plants in greenhouses.

2. Materials and methods

2.1. Experimental design and conditions

2.1.1. Experimental design

The experiments consisted of two [CO_2] and three drought treatments, which were arranged in a randomized complete block design. The [CO_2] treatments included an ambient concentration of approximately 400 μmol mol^{-1} (designated A) and an elevated concentration of (800 ± 20) μmol·mol^{-1} (designated E). Each [CO_2] treatment was replicated in two open-top greenhouses (area 36 m^2, ridge height 2.6 m). Two open-top greenhouses were supplied with CO_2 from a compressed CO_2 gas cylinder, and maintained at (800 ± 20) μmol·mol^{-1} controlled by an environmental control system (Auto Company, Beijing, China). The other two greenhouses were maintained at the ambient [CO_2]. The drought treatments consisted of control condition (nutrient solution; designated 0), moderate drought stress (nutrient solution + 5% polyethylene glycol (PEG) 6000; designated 1), and severe drought stress (nutrient solution + 10% PEG 6000; designated 2). Each drought treatment was replicated in four plastic containers placed inside the open-top greenhouses under each [CO_2] treatment condition.

2.1.2. Plant materials and growth conditions

Cucumber (*Cucumis sativus* L. cv Jinyou No. 35) seeds were rinsed in distilled water. They were subsequently imbibed in water for 6–8 h, and then germinated at 28 °C for about 1 d in darkness. The seeds were then sown in fifty holes with plugs and incubated in the greenhouse. The plugs (width, 26.5 cm; length, 52.3 cm) contained a 31:1: (volume ratio) mixture of peat, perlite, and vermiculite. Representative seedlings with one true leaf were transplanted and cultured hydroponically in darkened plastic containers (length, 35 cm; width, 28 cm; height, 12 cm; six plants per container). Twelve containers were placed randomly in each open-top greenhouse. We used full-strength Yamazaki cucumber nutrient solution (1.0 mM $NH_4H_2PO_4$, 3.5 mM Ca$(NO_3)_2{\cdot}4H_2O$, 6.0 mM KNO_3, 2.0 mM $MgSO_4{\cdot}7H_2O$, and full-strength trace elements). The electrical conductivity and pH of the nutrient solutions were maintained at 2.2–2.5 mS cm^{-1} and 6.8–7.0, respectively. Additionally, they were aerated every 5 min using air pumps, replenished to the original volumes daily, and refreshed every 3 d. Leaves were harvested after 5 d treatments for physiological analyses and for isolating chloroplasts. Each treatment consisted of three independent biological replicates.

2.2. Morphological indices and relative water content measurements

Plant height was measured as the distance from the stem base to the highest growing point. The hypocotyl diameter was measured using a vernier caliper. Leaf area was calculated based on the quadratic sum of the length of all fully expanded leaves. We measured the fresh weight (W_f), then dry weight (W_d) based on the weight of leaves after heating at 150–160 °C for 1 h, while the saturated fresh weight (W_t) was determined as the constant weight of leaves after soaking in distilled water for 70 min. The relative water content (RWC; %) was calculated as follows: $(W_f - W_d)/(W_t - W_d) \times 100$.

2.3. The chlorophyll a fluorescence transient

The chlorophyll *a* fluorescence transient (JIP-test) was measured using a Handy PEA chlorophyll fluorimeter (Hansatech Instruments Ltd, United Kingdom). The chlorophyll *a* fluorescence was induced with a 1-s red light treatment (3000 μmol m^{-2} s^{-1}). Each transient was standardized and analyzed according to Strasser's method (Appenroth et al., 2001). The O-step and P-step represent the minimum and maximum fluorescence intensities, respectively. The fluorescence intensities at 300 μs (K-step), 2 ms (J-step), and 30 ms (I-step) were also detected in the transient.

2.4. Measurement of malondialdehyde content and activity of antioxidant enzymes

All samples were prepared for malondialdehyde (MDA) and enzyme analyses by homogenization of the fresh tissue in a solution (4 mL g^{-1} fresh weight) containing 50 mM KH_2PO_4/K_2HPO_4 (pH 7.8), 1% PVP, 0.2 mM EDTA and 1% Triton X-100, using a mortar and pestle. After the homogenate was centrifuged at 12000 × *g* for 20 min at 4 °C, the supernatant was used to determine the enzyme activities (Cho and Park, 2000). All of the spectrophotometric analyses were conducted using an UV–visible spectrophotometer (UV-2450, Shimadzu, Japan). MDA content was determined using TBA colorimetric method (Heath and Packer, 1968); superoxidase dismutase (SOD) enzyme activity was measured by NBT reduction method (Beyer and Fridovich, 1987); peroxidase (POD) enzyme activity was measured by method of Omran (1980); catalase (CAT) enzyme activity was analyzed according to the method of Chance and Maehly (1955); ascorbate peroxidase (APX) enzyme activity was analyzed by the method of Nakano and Asada (1981).

2.5. Measurement of GSH, ASA and osmolytes

The content of reduced glutathione (GSH) and ascorbic acid (ASA) was measured by the method of Wang et al., 2004. Proline content was determined according to the ninhydrin coloration method (Bates et al., 1973). Soluble sugars were determined by the anthrone method and soluble proteins were determined by Coomassie brilliant blue G-250 method (Irigoyen et al., 1992).

2.6. Quantitative proteomics analyses of chloroplast

2.6.1. Protein extraction

Intact chloroplasts were isolated from leaves using Chloroplast

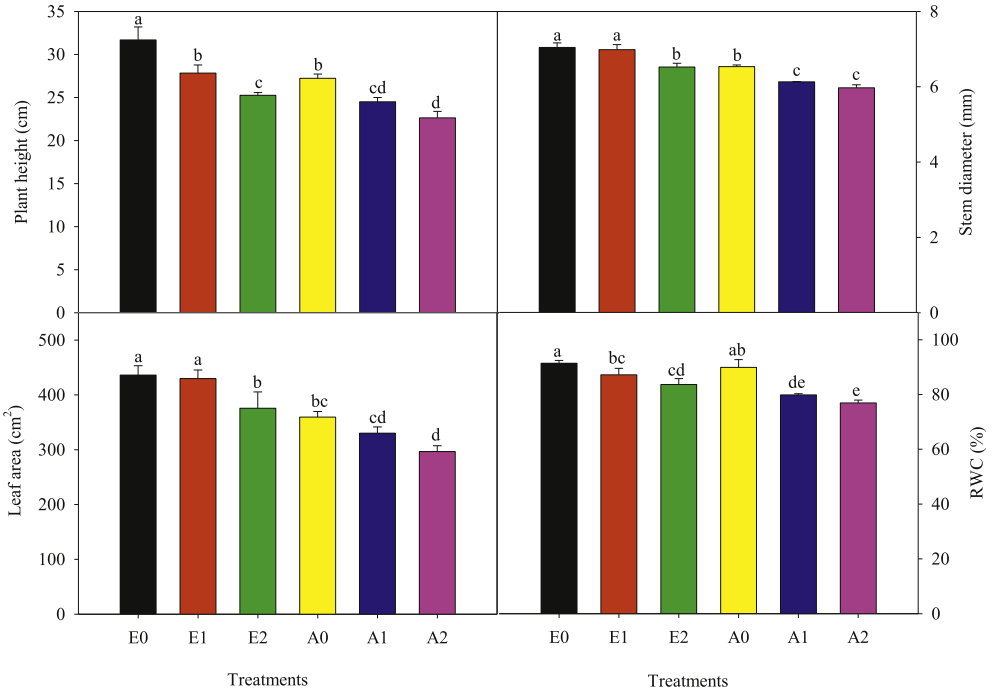

Fig. 1. Effects of drought stresses and E[CO_2] on the morphological indices and relative water content (RWC) of cucumber seedlings. E0, E[CO_2] + control; E1, E[CO_2] + moderate drought stress; E2, E[CO_2] + severe drought stress; A0, A[CO_2] + control; A1, A[CO_2] + moderate drought stress; A2, A[CO_2] + severe drought stress. Same as belows.

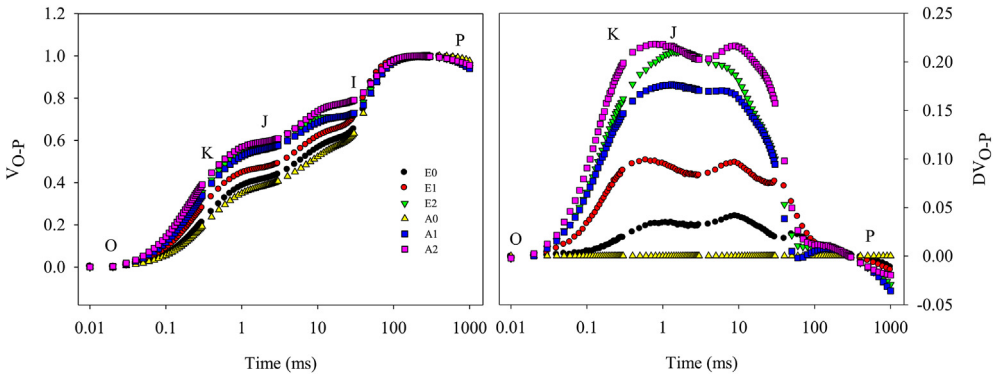

Fig. 2. Effects of drought stresses and E[CO_2] on chlorophyll *a* relative variable fluorescence parameters intensity (V_{o-p}) and the difference of relative variable fluorescence parameters intensity (ΔV_{o-p}) of cucumber seedlings.

Isolation Kit (Sigma). We then added 200 μL SDT buffer (4% SDS, 100 mM DTT, and 150 mM Tris-HCl, pH 8.0) to those chloroplasts. The suspension was boiled in water for 3 min, sonicated (10 times at 80 W for 10 s with intervals of 15 s), and then incubated at 100 °C for 3 min. The crude extract was centrifuged at 13,000 × *g* at 25 °C for 10 min. Protein abundance was determined using the BCA Protein Assay Reagent (Promega, USA), after which the supernatants were stored at −80 °C until used.

2.6.2. Protein digestion and iTRAQ labeling

Proteins were digested using the filter aided proteome preparation procedure as previously described (Wiśniewski et al., 2009). The resulting peptide mixture was labeled using the 8-plex iTRAQ reagent according to the manufacturer's instructions (Applied Biosystems). Briefly, for each sample, 200 μg proteins were prepared in 30 μL STD buffer. The detergent, DTT, and other low molecular weight components removed using UA buffer (8 M urea and 150 mM Tris-HCl, pH 8.0) and repeated ultrafiltration (10 kDa molecular weight cut-off; Pall). We then added 100 μL 0.05 M iodoacetamide (prepared in UA buffer) to block reduced cysteine residues, and the samples were incubated for 20 min in darkness. The filters were washed three times with 100 μL UA buffer and then two times with 100 μL DS buffer (50 mM triethylammonium bicarbonate, pH 8.5). Finally, the protein suspensions were digested with 2 μg trypsin (Promega) in 40 μL DS buffer overnight at 37 °C. The resulting peptides were collected as a filtrate. The peptide content was estimated according to the UV light spectral density at 280 nm. We used an extinction coefficient of 1.1 for a 0.1% (g·L^{-1}) solution, which was calculated based on the frequency of tryptophan and tyrosine in vertebrate proteins.

For labeling, each iTRAQ reagent was dissolved in 70 μL ethanol and added to the peptide mixtures. The samples were labeled as (A0) −113, (A1) −114, (A2) −115, (E0) −116, (E1) −117, (E2) −118, and (IS)-119, and then multiplexed and vacuum-dried.

2.6.3. Peptide fractionation by strong cation exchange chromatography

The iTRAQ-labeled peptides were fractionated by strong cation exchange chromatography using the AKTA Purifier system (GE Healthcare). The dried peptide mixture was reconstituted and acidified with 2 mL buffer A (10 mM KH_2PO_4 in 25% acetonitrile, pH 2.7), and then loaded onto a Poly SULFOETHYL 4.6 × 100 mm column (5 μm, 200 Å; PolyLC Inc., Maryland, USA). The peptides were eluted at a flow rate of 1 mL min^{-1} with a gradient of 0–10% buffer B (500 mM KCl and 10 mM KH_2PO_4 in 25% acetonitrile, pH 2.7) for 2 min, 10–20% buffer B for 25 min, 20–45% buffer B for 5 min, and 50–100% buffer B for 5 min.

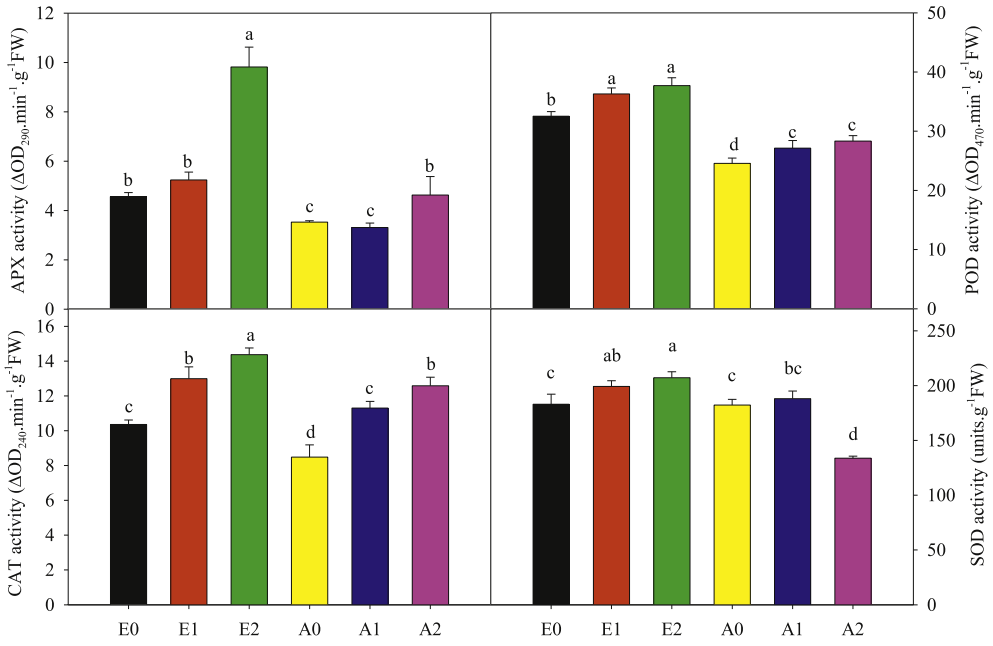

Fig. 3. Effects of drought stresses and E[CO_2] on the antioxidant enzyme activity of cucumber seedlings.

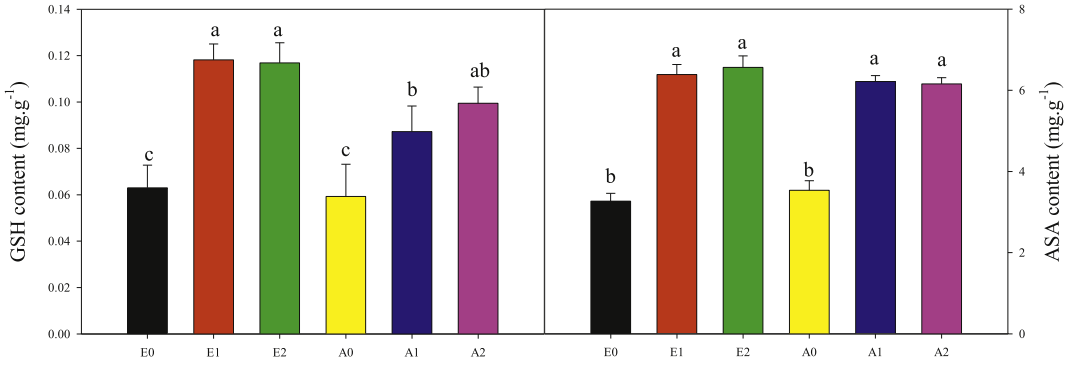

Fig. 4. Effects of drought stresses and E[CO_2] on GSH and ASA contents of cucumber seedlings.

The elution was monitored by absorbance at 214 nm, and fractions were collected every 1 min for a total of about 33. These fractions were combined into 12 pools, and then desalted using Empore™ SPE Cartridges C18 (standard density; 7 mm bed ID and 3 ml volume; Sigma). Each fraction was concentrated by vacuum centrifugation and reconstituted in 40 µL 0.1% (v/v) trifluoroacetic acid. All samples were stored at −80 °C until analyzed by liquid chromatography–tandem mass spectrometry.

2.6.4. Liquid chromatography–electrospray ionization tandem mass spectrometry analysis

Experiments were performed using a Q Exactive mass spectrometer coupled to the Easy nLC system (Thermo Fisher Scientific). A 10-µL aliquot of each fraction was analyzed by nanoLC-MS/MS. The peptide mixture (5 µg) was loaded onto a C18-reversed phase column (length, 15 cm; inner diameter, 75 µm) packed in-house with RP-C18 5-µm resin in buffer A (0.1% formic acid). The peptides were separated with a linear gradient of buffer B (80% acetonitrile and 0.1% formic acid) at a flow rate of 250 nL min^{-1} (controlled by IntelliFlow technology) over 140 min. Mass spectrometry data were obtained using a data-dependent Top 10 method, in which the most abundant precursor ions from the survey scan (300–1800 m·z^{-1}) were selected for HCD fragmentation. The target value was determined based on the predictive Automatic Gain Control. The dynamic exclusion duration was 60 s. Survey scans were generated at a resolution of 70000 (m·z^{-1} 200), while the resolution setting for HCD spectra was 17500 (m·z^{-1} 200). The normalized collision energy was 30 eV, and the underfill ratio, which specifies the minimum percentage of the target value likely to be reached at the maximum fill time, was defined as 0.1%. The instrument was run with the peptide recognition mode enabled.

2.6.5. Sequence database search and data analysis

The MS/MS spectra were analyzed using the Mascot search engine (Matrix Science, London, UK; version 2.2) of Proteome Discoverer 1.4 (Thermo Electron, San Jose, CA, USA). We searched the UniProt Cucumber database (24636 sequences downloaded September 22, 2016) and the decoy database. The following parameters were used to identify proteins: Peptide mass tolerance, 20 ppm; MS/MS tolerance, 0.1 Da; Enzyme, trypsin; Missed cleavage, 2; Fixed modifications, Carbamidomethyl (C), iTRAQ8plex (K), and iTRAQ8plex (N-term); Variable modification, Oxidation (M) and FDR ≤ 0.01 (Sandberg et al., 2012).

2.6.6. Bioinformatics

The Gene Ontology (GO) program Blast2GO (https://www.blast2go.com/) was used to annotate differentially expressed proteins (DEPs), which were used to create histograms of GO annotations (i.e., cell component, biological process, and molecular function) (Götz et al., 2008). For pathway analyses, the DEPs were mapped to the terms in the Kyoto Encyclopedia of Genes and Genomes database using theKAAS

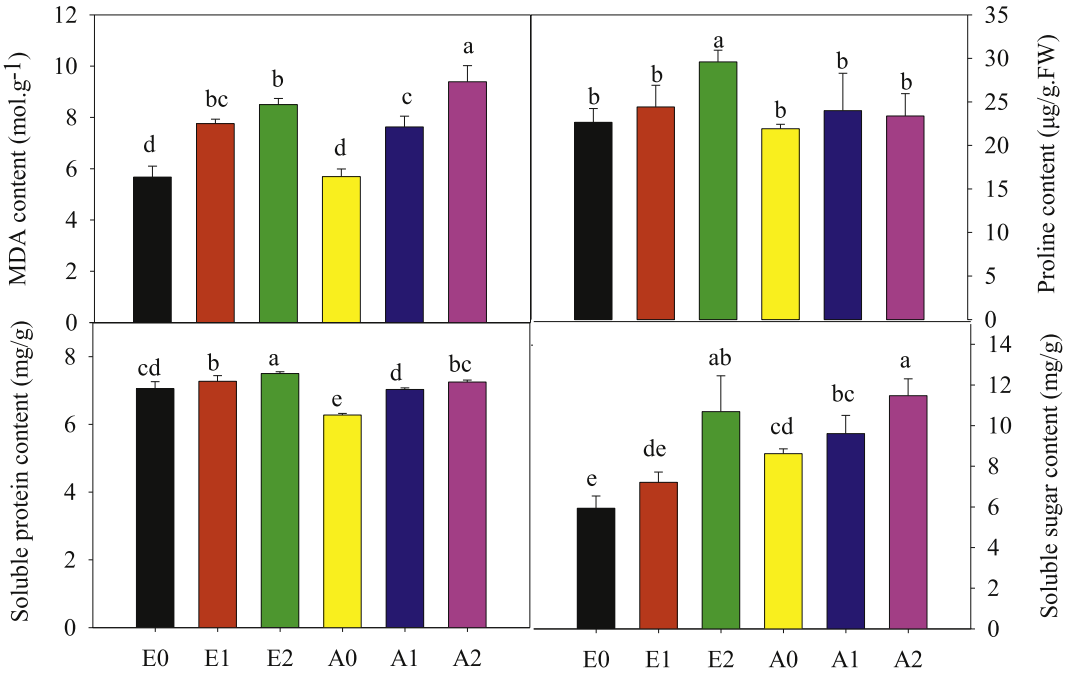

Fig. 5. Effects of drought stresses and E[CO_2] on MDA, proline, soluble protein and soluble sugar contents of cucumber seedlings.

Table 1
Protein identification result statistics.

Category	Number
Total spectra	688981
Spectra	112963
Peptide	8589
Unique peptide	8063
Protein	2046

program (Kanehisa et al., 2012) (http://www.genome.jp/kaas-bin/kaas_main).

2.7. Statistical analyses

Data are presented as the mean ± standard deviation of three replicates. The statistical analyses were completed using the DPS software. Duncan's multiple range tests were applied to compare the significant differences ($p < 0.05$) between treatments.

3. Results

3.1. Morphological and photochemistry efficiency of cucumber seedlings in response to drought stresses and E[CO_2]

Moderate and severe drought stress significantly decreased plant height, stem diameter, leaf area, and relative water content (RWC) of cucumber seedlings under A[CO_2], E[CO_2] significantly increased these morphological parameters and RWC of cucumber seedlings under drought stresses (Fig. 1). Compared with A[CO_2], E[CO_2] increased plant height by 13.6% and 11.6% under moderate and severe drought stress conditions, respectively; increased stem diameter by 13.9% and 9.2% under moderate and severe drought stress conditions, respectively; increased leaf area by 30.2% and 26.7% under moderate and severe drought stress conditions, respectively; increased RWC by 9.2% and 8.8% under moderate and severe drought stress conditions, respectively. Therefore, E[CO_2] can alleviate drought stress through promoting growth and maintaining water balance in seedlings.

The fast chlorophyll fluorescence induction kinetics curve (JIP-test) based on the theory of energy fluxes in biomembranes has been widely used to analyze the chlorophyll *a* fluorescence kinetics transient helping researchers to have a deeper insight into the primary photochemical reaction in the photosynthetic apparatus. From Fig. 2, moderate and severe drought stress significantly increased the J and K peaks of kinetic curves of rapid chlorophyll fluorescence induction, while they were decreased by E[CO_2], especially under moderate drought stress, which indicate that E[CO_2] can alleviate the damage of photosynthetic electron transport chain caused by drought stresses.

3.2. Antioxidant system of cucumber seedlings in response to drought stresses and E[CO_2]

According to Fig. 3, drought stress increased the activities of APX, POD and CAT, E[CO_2] significantly increased the activities of APX, POD, and CAT under all three of the water conditions. Also E[CO_2], significantly increased the activity of SOD under moderate and severe drought stress.

GSH and ASA contents under moderate and severe drought stress were significantly higher than that of control, but the differences between them were not significant (Fig. 4). Although E[CO_2] increased GSH and ASA contents under moderate and severe drought stress, only GSH content in moderate drought stress was significantly different.

According to Fig. 5, a gradual increase in MDA content was detected in cucumber leaves as drought stress getting severer under both A[CO_2] and E[CO_2]. And there was a significant decrease of MDA content under E[CO_2] when cucumber seedlings exposed to severe drought stress. Proline, soluble protein and soluble sugar content were increased as drought stress getting severer. E[CO_2] significantly increased the content of soluble protein and proline under severe drought stress. Soluble sugar content under E[CO_2] was lower than that under A[CO_2].

3.3. iTRAQ-based proteomic analyses of chloroplast protein patterns under different [CO_2] and drought stresses conditions

Table 1 presents the protein identification statistics after the MS/MS data were analyzed with the Mascot search engine (filter condition: peptide FDR ≤ 0.01). We identified 688981 total spectra, 112963 spectra matched to known spectra, 8589 peptides, 8063 unique

Table 2
Differentially expressed cucumber chloroplast proteins under E[CO_2] and drought stresses.

Accession[a]	Proteinname	Cov[b]	UP[c]	MW[d][kDa]	pI[e]	A1/A0[f]	A2/A0[f]	E1/E0[f]	E2/E0[f]	E0/A0[f]	E1/A1[f]	E2/A2[f]
Pigment biosynthesis												
A0A0A0KI79	Magnesium-chelatase subunit ChlI-2	26.9	10	45.73	6.00	1.18 ± 0.00	1.35 ± 0.00	0.68 ± 0.00	0.61 ± 0.00	1.53 ± 0.00	0.89 ± 0.00	0.69 ± 0.00
A0A0A0KM90	Uroporphyrinogen decarboxylase 2	2.04	1	43.03	8.62	1.02 ± 0.80	1.16 ± 0.19	0.79 ± 0.03	0.64 ± 0.00	1.11 ± 0.00	0.86 ± 0.27	0.60 ± 0.03
A0A0A0KCD2	Tetrapyrrole-binding protein	2.69	1	28.98	7.21	0.92 ± 0.25	1.23 ± 0.15	0.51 ± 0.04	0.64 ± 0.06	1.06 ± 0.62	0.59 ± 0.02	0.55 ± 0.03
A0A0A0KV99	Probable carotenoid cleavage dioxygenase 4	17.77	10	65.00	6.24	0.97 ± 0.43	0.84 ± 0.01	0.96 ± 0.32	1.46 ± 0.00	0.89 ± 0.05	0.89 ± 0.02	1.56 ± 0.00
A0A0A0KZP8	Magnesium-chelatase subunit ChlH	5.5	7	153.52	6.24	0.93 ± 0.47	0.92 ± 0.36	0.63 ± 0.00	0.74 ± 0.01	1.20 ± 0.14	0.82 ± 0.04	0.96 ± 0.17
A0A0A0KZN7	Protochlorophyllide reductase A	56.89	21	43.15	8.79	0.66 ± 0.00	0.68 ± 0.00	0.72 ± 0.00	0.80 ± 0.00	0.89 ± 0.00	0.97 ± 0.25	1.05 ± 0.08
A0A0A0KIH3	Carotene epsilon-monooxygenase	23.43	11	62.41	6.99	0.60 ± 0.00	0.63 ± 0.00	0.86 ± 0.00	0.86 ± 0.00	0.76 ± 0.00	1.08 ± 0.10	1.04 ± 0.11
A0A0A0LJK3	Zeaxanthin epoxidase	30.38	21	73.13	6.95	0.66 ± 0.00	0.63 ± 0.00	1.00 ± 0.89	1.02 ± 0.53	0.71 ± 0.00	1.06 ± 0.12	1.14 ± 0.01
A0A0A0KVC2	Phytoene synthase	2.58	1	43.82	8.57	0.62 ± 0.00	0.63 ± 0.01	0.68 ± 0.01	0.86 ± 0.06	0.80 ± 0.01	0.89 ± 0.35	1.10 ± 0.46
A0A0A0L5K4	Protein LUTEIN DEFICIENT 5	15.06	8	69.69	6.87	0.59 ± 0.01	0.68 ± 0.01	0.67 ± 0.00	0.66 ± 0.00	0.97 ± 0.69	1.11 ± 0.34	0.95 ± 0.49
Photosynthesis												
A0A0A0KBL8	Transketolase-2	9.66	3	80.51	7.11	1.50 ± 0.02	1.73 ± 0.02	0.93 ± 0.12	1.20 ± 0.01	1.00 ± 0.96	0.62 ± 0.01	0.69 ± 0.04
A0A0A0LAW4	Photosystem I reaction center subunit VI-2	18.06	4	15.24	9.91	0.58 ± 0.00	0.63 ± 0.00	1.03 ± 0.22	0.74 ± 0.00	0.88 ± 0.00	1.56 ± 0.00	1.04 ± 0.19
Q4VZH7	Photosystem II reaction center protein L	39.47	2	4.49	4.50	0.52 ± 0.00	0.48 ± 0.00	0.96 ± 0.42	0.30 ± 0.00	1.37 ± 0.00	2.56 ± 0.00	0.86 ± 0.19
A0A0A0LA49	Early light-induced protein 1	24.48	3	20.20	9.51	1.74 ± 0.00	2.03 ± 0.00	2.22 ± 0.00	1.18 ± 0.01	0.99 ± 0.90	1.27 ± 0.03	0.58 ± 0.00
A0A0A0LX23	Chlorophyll *a-b* binding protein	54.72	2	28.25	5.43	1.15 ± 0.03	1.13 ± 0.06	0.97 ± 0.49	0.80 ± 0.00	1.54 ± 0.00	1.30 ± 0.00	1.08 ± 0.05
Q2QD75	Photosystem II reaction center protein J	17.5	1	4.14	6.23	0.73 ± 0.13	0.60 ± 0.02	0.40 ± 0.00	0.36 ± 0.00	1.95 ± 0.00	1.06 ± 0.72	1.16 ± 0.23
A0A0A0LY43	Rubisco accumulation factor 1.1	9.78	5	49.42	5.06	1.05 ± 0.14	1.11 ± 0.05	0.53 ± 0.00	0.50 ± 0.00	1.48 ± 0.00	0.76 ± 0.00	0.67 ± 0.00
A0A0A0LAD3	Ferredoxin-2	6.76	1	16.29	4.81	1.72 ± 0.15	1.29 ± 0.23	1.11 ± 0.39	1.30 ± 0.03	1.54 ± 0.06	0.99 ± 0.96	1.55 ± 0.01
Q2QD78	Photosystem I assembly protein Ycf4	18.48	5	21.63	9.80	0.55 ± 0.00	0.62 ± 0.00	0.72 ± 0.00	0.64 ± 0.00	0.91 ± 0.00	1.20 ± 0.01	0.94 ± 0.13
G3EIX4	NAD(P)H-quinone oxidoreductase subunit 1	8	2	35.59	9.25	0.53 ± 0.00	0.69 ± 0.00	1.04 ± 0.76	1.84 ± 0.00	0.47 ± 0.00	0.92 ± 0.58	1.26 ± 0.01
A0A0A0KLW9	Ribulose bisphosphate carboxylase/oxygenase activase	63.43	15	48.29	8.13	1.05 ± 0.03	1.28 ± 0.00	0.72 ± 0.00	0.61 ± 0.00	1.42 ± 0.00	0.96 ± 0.03	0.68 ± 0.00
Stress and defenseresponse												
Q96398	Probable plastid-lipid-associated protein 1	37.27	11	35.22	5.15	1.67 ± 0.00	1.56 ± 0.00	1.81 ± 0.00	2.04 ± 0.00	0.96 ± 0.04	1.04 ± 0.06	1.25 ± 0.00
A0A0A0K3W6	Cysteine proteinase inhibitor 4	47.03	11	23.45	8.69	2.72 ± 0.00	2.38 ± 0.00	1.87 ± 0.00	1.55 ± 0.00	1.10 ± 0.05	0.75 ± 0.00	0.71 ± 0.00
A0A0A0KLY3	PLAT domain-containing protein 1	5.36	1	18.34	4.88	1.78 ± 0.00	2.00 ± 0.00	1.45 ± 0.00	1.91 ± 0.00	1.07 ± 0.25	0.87 ± 0.01	1.02 ± 0.44
A0A0A0L683	GrpE protein homolog	31.05	8	33.48	6.90	0.60 ± 0.00	0.62 ± 0.00	1.03 ± 0.47	1.56 ± 0.00	0.42 ± 0.00	0.73 ± 0.00	1.07 ± 0.05
A0A0A0KQ14	25.3 kDa heat shock protein	27.51	5	25.49	9.14	1.60 ± 0.00	1.37 ± 0.00	1.16 ± 0.07	1.04 ± 0.60	1.09 ± 0.23	0.79 ± 0.00	0.83 ± 0.01
Q9SXL8	MLP-like protein 43	17.88	2	17.52	6.79	1.95 ± 0.00	1.32 ± 0.00	1.38 ± 0.00	1.59 ± 0.00	0.93 ± 0.29	0.66 ± 0.00	1.12 ± 0.00
A0A0A0K281	Cysteine proteinase inhibitor 1	34.85	4	14.41	8.78	3.44 ± 0.00	1.79 ± 0.00	1.88 ± 0.00	1.29 ± 0.01	1.06 ± 0.54	0.58 ± 0.00	0.76 ± 0.00
A0A0A0LYF4	Cysteine proteinase inhibitor 5	12.44	3	23.11	7.64	2.74 ± 0.00	2.60 ± 0.00	2.47 ± 0.00	1.58 ± 0.00	1.11 ± 0.07	1.00 ± 0.96	0.67 ± 0.00
A0A0A0KTF5	25.3 kDa heat shock protein	37.93	10	26.31	8.92	1.70 ± 0.00	1.83 ± 0.00	0.78 ± 0.00	0.52 ± 0.00	1.75 ± 0.00	0.80 ± 0.02	0.50 ± 0.00
A0A0A0K8V5	Acyl carrier protein 4	6.34	1	15.16	4.81	0.83 ± 0.00	1.18 ± 0.01	1.29 ± 0.01	1.23 ± 0.01	0.66 ± 0.00	1.03 ± 0.33	0.69 ± 0.00
A0A0A0LAP9	Late embryogenesis abundant protein-like	2.54	2	60.34	6.58	4.21 ± 0.03	2.33 ± 0.01	2.81 ± 0.01	2.55 ± 0.02	1.04 ± 0.87	0.70 ± 0.15	1.14 ± 0.08
A0A0A0L2P8	Glutathione S-transferase F10	16.36	4	42.74	5.22	1.55 ± 0.04	1.47 ± 0.05	0.93 ± 0.65	1.09 ± 0.24	1.15 ± 0.38	0.69 ± 0.07	0.85 ± 0.09
A0A0A0KZN3	NADPH-dependent aldo-keto reductase	4.19	1	21.79	6.54	1.04 ± 0.37	0.91 ± 0.20	0.90 ± 0.25	1.09 ± 0.29	0.77 ± 0.05	0.66 ± 0.01	0.92 ± 0.21
Redox homeostasis												
A0A0A0LUA8	Aldehyde dehydrogenase family 2 member B4	36.31	19	59.55	7.56	0.57 ± 0.00	0.68 ± 0.00	1.08 ± 0.07	1.74 ± 0.00	0.44 ± 0.00	0.84 ± 0.00	1.13 ± 0.00
A0A0A0LSY7	CBS domain-containing protein CBSX1	7.23	1	25.65	7.39	1.70 ± 0.00	1.55 ± 0.00	0.84 ± 0.00	0.90 ± 0.02	1.21 ± 0.01	0.60 ± 0.00	0.70 ± 0.00
A0A0A0KJ06	ABC transporter-like	14.06	10	86.17	9.01	0.88 ± 0.00	0.87 ± 0.00	0.76 ± 0.00	0.58 ± 0.00	1.40 ± 0.00	1.22 ± 0.00	0.94 ± 0.07
A0A0A0KNX7	Probable phospholipid hydroperoxide glutathione peroxidase 6	15.77	4	26.83	9.20	1.60 ± 0.00	1.34 ± 0.03	1.40 ± 0.01	1.41 ± 0.02	0.89 ± 0.33	0.78 ± 0.00	0.94 ± 0.47
A0A0A0KM69	Ferritin-2	22.01	5	28.99	5.30	1.96 ± 0.00	2.23 ± 0.00	1.19 ± 0.03	1.46 ± 0.01	1.21 ± 0.05	0.73 ± 0.03	0.79 ± 0.02
A0A0A0K8M3	2Fe–2S ferredoxin-like superfamily protein	13.41	2	18.47	9.10	0.71 ± 0.01	0.85 ± 0.05	1.12 ± 0.30	1.40 ± 0.01	0.62 ± 0.00	0.97 ± 0.79	1.01 ± 0.88
A0A0A0KMC3	Thioredoxin O1	18.69	3	22.05	8.62	0.63 ± 0.04	0.78 ± 0.17	1.17 ± 0.48	1.89 ± 0.01	0.43 ± 0.02	0.81 ± 0.15	1.05 ± 0.53
A0A0A0LQK6	Thioredoxin family protein	5.92	2	40.02	8.25	0.78 ± 0.19	0.69 ± 0.11	0.81 ± 0.12	1.03 ± 0.25	1.10 ± 0.06	1.14 ± 0.55	1.66 ± 0.04
Metabolic pathways												
A0A0A0KXD3	ATP-dependent zinc metalloprotease FTSH 6	36.82	15	73.34	6.32	1.81 ± 0.00	1.65 ± 0.00	2.31 ± 0.00	1.36 ± 0.00	1.01 ± 0.61	1.29 ± 0.00	0.84 ± 0.00
A0A0A0KX20	Nucleoside diphosphate kinase IV	21.85	5	25.96	9.11	0.64 ± 0.00	0.75 ± 0.00	1.20 ± 0.06	1.98 ± 0.00	0.43 ± 0.00	0.81 ± 0.01	1.14 ± 0.00
A0A0A0L1W1	Lipoxygenase 2	5.82	2	43.91	6.89	1.44 ± 0.00	1.76 ± 0.00	1.31 ± 0.04	1.55 ± 0.01	0.97 ± 0.73	0.88 ± 0.07	0.85 ± 0.07
A0A0A0KX59	Enoyl-[acyl-carrier-protein] reductase [NADH]	19.69	7	41.38	8.44	1.31 ± 0.00	1.53 ± 0.00	1.22 ± 0.01	1.19 ± 0.03	0.92 ± 0.10	0.85 ± 0.00	0.72 ± 0.00
A0A0A0K9Z6	Bifunctional L-3-cyanoalanine synthase/cysteine synthase C1	39.47	13	40.32	7.94	0.62 ± 0.00	0.68 ± 0.00	0.97 ± 0.42	1.30 ± 0.00	0.59 ± 0.00	0.92 ± 0.25	1.13 ± 0.01
A0A0A0KBM9	Dehydrodolichyl diphosphate synthase 2	17.28	4	34.56	8.13	1.39 ± 0.00	1.57 ± 0.00	1.05 ± 0.07	0.92 ± 0.04	1.26 ± 0.00	0.95 ± 0.17	0.74 ± 0.00
A0A0A0L6H3	Ferredoxin–nitrite reductase	11.66	6	65.47	6.57	0.80 ± 0.00	0.79 ± 0.00	0.59 ± 0.00	0.56 ± 0.00	1.10 ± 0.02	0.81 ± 0.00	0.78 ± 0.00

(*continued on next page*)

Table 2 (*continued*)

Accession[a]	Proteinname	Cov[b]	UP[c]	MW[d] [kDa]	pI[e]	A1/A0[f]	A2/A0[f]	E1/E0[f]	E2/E0[f]	E0/A0[f]	E1/A1[f]	E2/A2[f]
A0A0A0KF41	Isocitrate dehydrogenase [NAD] catalytic subunit 5	19.89	6	40.73	7.91	0.73 ± 0.00	0.79 ± 0.00	1.16 ± 0.19	1.55 ± 0.00	0.56 ± 0.00	0.89 ± 0.09	1.09 ± 0.02
A0A0A0KKC3	Threonine dehydratase biosynthetic	9.59	5	67.30	6.39	1.28 ± 0.03	1.30 ± 0.02	1.26 ± 0.00	2.26 ± 0.00	0.87 ± 0.13	0.85 ± 0.03	1.51 ± 0.00
Q2QD64	Chloroplastic ATP-dependent Clp protease proteolytic subunit 1	12.82	3	21.54	5.34	1.07 ± 0.06	1.24 ± 0.01	0.88 ± 0.09	0.85 ± 0.05	0.97 ± 0.61	0.81 ± 0.00	0.67 ± 0.00
A0A0A0KUG3	Monodehydroascorbate reductase 4	5.81	3	50.57	7.91	0.54 ± 0.08	0.58 ± 0.10	1.09 ± 0.07	1.84 ± 0.05	0.40 ± 0.04	0.81 ± 0.35	1.27 ± 0.19
A0A0A0K785	Imidazole glycerol phosphate synthase hisHF	1.79	1	56.33	7.43	1.23 ± 0.09	1.35 ± 0.07	0.89 ± 0.33	0.99 ± 0.92	0.92 ± 0.39	0.66 ± 0.04	0.68 ± 0.03
A0A0A0LLU4	Probable N-acetyl-gamma-glutamyl-phosphate reductase	9	3	43.04	7.58	1.19 ± 0.33	1.28 ± 0.12	1.17 ± 0.00	1.09 ± 0.13	0.78 ± 0.16	0.77 ± 0.07	0.66 ± 0.00
A0A0A0M1E9	DEAD-box ATP-dependent RNA helicase 3	22.19	16	82.06	7.36	1.02 ± 0.52	1.07 ± 0.04	0.66 ± 0.00	0.70 ± 0.00	1.40 ± 0.00	0.91 ± 0.02	0.91 ± 0.02

[a] Database accession numbers.
[b] Coverage.
[c] Unique peptides.
[d] Theoretical mass (kDa).
[e] PI.
[f] Ratios of treatments ± P-value.

peptides, and 2046 proteins. To more stringently screen DEPs, we used a fold change > 1.5 ($p < 0.05$) as the cutoff.

In this study, we focused on the chloroplast differentially expressed proteins (DEPs) with important function and the highest confidence levels (Table 2 and Table S1). To visualize their expression patterns in response to E[CO_2] and drought stresses, we performed venn diagram, hierarchical clustering and functional classification to find associated changes of chloroplast proteins. From Fig. 6, there were no differential expression of chloroplast proteins under E[CO_2], while eight differential expressed proteins were observed under different water conditions. Hierarchical clustering analysis revealed that E[CO_2] changed proteins abundance under control and drought stress, and the number of down-regulated proteins was more than up-regulated proteins (Fig. 7). The chloroplast DEPs in response to E[CO_2] under both moderate and severe drought stress were functionally classified (Fig. 8). According to Fig. 8A, the DEPs under E[CO_2] were mainly associated with the metabolic pathway (17%), photosynthesis (15%), stress and defense responses (11%), the ribosome (11%), redox homeostasis (11%), and pigment biosynthesis (8%). These categories were also detected under moderate and severe drought stress (Fig. 8B–C), 42% of the DEPs in cucumber seedlings exposed to severe drought stress were related to the ribosome (Fig. 8C), suggesting that drought stress altered ribosome formation in chloroplasts, which further affected protein synthesis.

4. Discussion

4.1. Proteins involved in pigment biosynthesis and photosynthesis

Pathways of DEPs involved in pigment biosynthesis and photosynthesis were diagrammatized in Fig. 9. In this study, protochlorophyllide reductase A (PCRA), tetrapyrrole-binding protein (TB), magnesium-chelatase subunit ChlH (ChlH), magnesium-chelatase subunit ChlI-2 (ChlI-2), and uroporphyrinogen decarboxylase 2 (UPD2) were identified as chlorophyll biosynthetic proteins. The contents of PCRA and TB decreased considerably after the moderate drought treatment. The ChlH was down-regulated under moderate drought conditions, while the ChlI-2 was down-regulated under severe drought conditions. The decreased abundance of these enzymes suggested that chlorophyll biosynthesis was inhibited in drought-stressed plants. The loss of chlorophyll under drought stresses might decrease photons absorption of leaves, leading to enhanced photoprotective and antioxidant capacities of leaves related to the number of photon absorption (Munné-Bosch and Alegre, 2000). Additionally, we found that the abundance of ChlI-2 increased significantly at E[CO_2] in the absence of drought stress. In contrast, E[CO_2] decreased the abundance of UPD2 under severe drought stress and tetrapyrrole-binding protein under both moderate and severe stress. These findings suggested that E[CO_2] promoted the synthesis of chlorophyll in the absence of drought stress, but reduced the synthesis of chlorophyll under drought stress.

Four proteins associated with carotenoid biosynthesis were identified in this study. They were carotene epsilon-monooxygenase (CEM), protein LUTEIN DEFICIENT 5 (PLD5), phytoene synthase (PSY) and zeaxanthin epoxidase (ZEP). The abundance of the four proteins was down-regulated under moderate and severe drought conditions, especially under the A[CO_2]. This implied that although carotene was one of the most important metabolites in plant antioxidant defense system, it was very susceptible to oxidative destruction caused by water deficit stress (Jaleel et al., 2009). Furthermore, the abundance of ZEP decreased in drought stressed plants, resulted in lowered violaxanthin contents, which ultimately decreased the number of photons absorbed by leaves, thereby alleviating photodamages due to water deficit stress.

Photosynthesis is the primary process adversely affected by drought stress (Ghotbi-Ravandi et al., 2014). We observed that most proteins related to photosynthetic light reaction and electron transfers were down-regulated when plants were exposed to moderate and severe

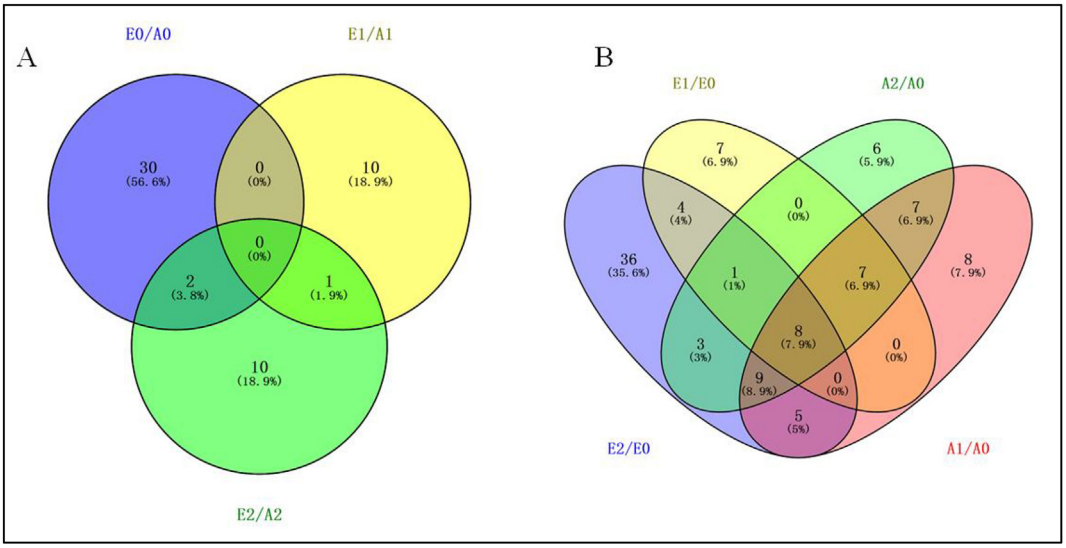

Fig. 6. Venn diagram analysis of the differentially expressed chloroplast proteins with max confidence from cucumber seedlings for E[CO_2] (A) and drought stresses (B).

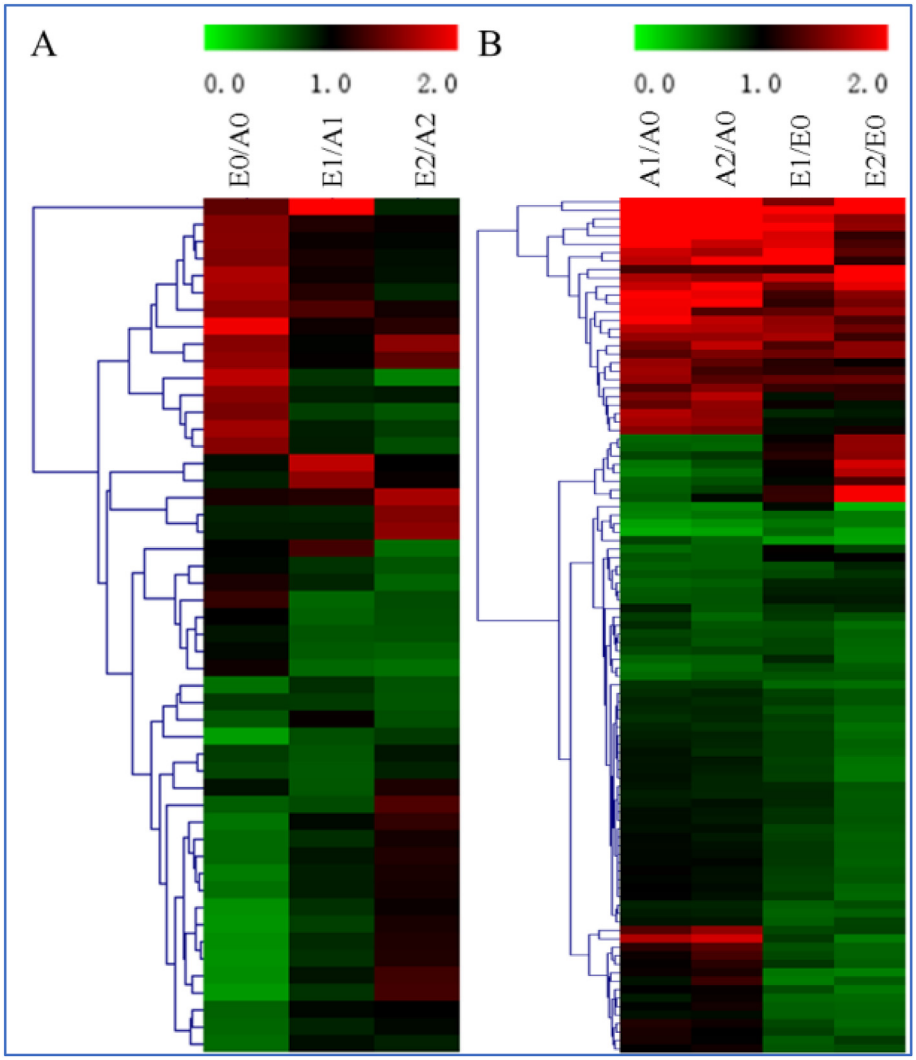

Fig. 7. Hierarchical clustering analysis of the differentially expressed chloroplast proteins with max confidence from cucumber seedlings for E[CO2] (A) and drought stresses (B). The rows represent individual proteins. The proteins that increased and decreased in abundance are indicated in red and green, respectively. (For interpretation of the references to color in this figure legend, the reader is referred to the Web version of this article.)

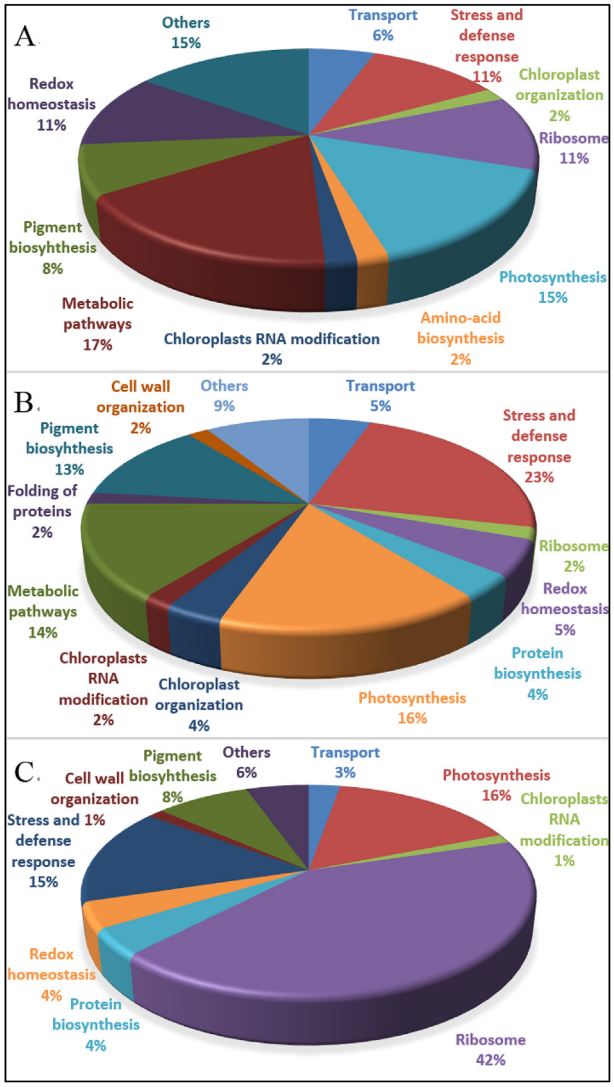

Fig. 8. Functional classification of differentially expressed proteins (DEPs) identified in chloroplast of cucumber seedlings under E[CO_2] (A), moderate drought stress (B) and severe drought stress (C). The classification is based on KEGG (http://www.kegg.jp/kegg/pathway.html).

drought stress. PSII reaction center proteins L and J (psbL and psbJ) and chlorophyll *a/b*-binding protein (CHlB) were down-regulated under moderate and severe drought conditions (Table 2). This suggested that drought stress led to PSII structural damages that inhibited light-harvesting and electron transfers. PSI assembly protein Ycf4 (YCF4) and PSI reaction center subunit VI-2 (VI-2) contents were considerably down-regulated under drought conditions (Table 2), indicating that drought stress decreases PSI protein quantity and integrity. Additionally, the abundance of RuBisCO accumulation factor 1.1 (RuBisCO AF) decreased under drought conditions. Many studies have concluded that E[CO_2] could increase plant photosynthesis under drought stress (Chen et al., 2015; Hao et al., 2016). Our previous research showed that E[CO_2] significantly increased photosynthetic rate under moderate and severe drought stress (Liu et al., 2017). E[CO_2] increased the abundance of psbL and CHlB of PSII in seedlings grown in nutrient solution. Similar results were observed for psbJ and VI-2 in seedlings exposed to moderate drought stress. These results indicated that E[CO_2] enhanced electron transfers and photosystem stability, which might increase photosynthetic activities under moderate drought conditions. In response to severe drought stress, we observed that E[CO_2] increased the abundance of ferredoxin-2 (Fd) and decreased the abundance of RuBisCO AF. Ferredoxin serving as an electron transfer bifurcation point, and increased in its abundance, which might indicate that more types of electron transport were involved in photosynthetic activities under severe drought conditions at relatively high [CO_2]. Additionally, our results suggested that RuBisCO assembly or stability were affected by E[CO_2] under severe drought conditions. Decreases in RuBisCO activity in leaves at E[CO_2] were caused by decreased activase activity, possibly in response to unfavorable ATP/ADP ratios (Crafts-Brandner and Salvucci, 2000).

4.2. Proteins involved in stress and defense responses

The stimulation of stress can trigger pathways more than one, therefore we characterized and analyzed stress and defense response proteins. Probable plastid-lipid-associated protein may be involved in stress-related jasmonate (JA) biosynthesis and contributes to the protection of PSII against light stress (Youssef et al., 2010). JA can improve plants resistance, and plants are vulnerable to light stress caused by excess light energy under drought stress. These indicate that an increase in the abundance of probable plastid-lipid-associated protein can improve cucumber's resistance to drought stress and protect PSII against light stress. PLAT domain-containing protein is a positive regulator of abiotic stress tolerance involved in the regulation of plant growth and may be a downstream target of the abscisic acid (ABA) signaling pathway (Hyun et al., 2013). In this study, drought stresses up-regulated probable plastid-lipid-associated protein and PLAT domain-containing protein, which might enhance the resistance of cucumber to drought. We found an up-regulation of Late embryogenesis abundant protein-like (LEA), which might be involved in protecting plants subjected to drought stress and helping plants adapting and surviving in drought condition (Costa et al., 2015). Previous studies had reported that higher of RWC, SOD and POD activities, and photosystem II activity were found in transgenic tobacco that ectopically express BhLEA1 and BhLEA2 were higher than wild-type plants (Nakayama et al., 2008). Our results also showed that drought stresses up-regulated LEA protein as well as SOD and POD activities (except A2 treatment). This further implied that LEA protein could prevent enzymes from inactivating. Under A[CO_2] conditions, SOD activity decreased after severe drought treatment, which probably because the drought stress was too severe for the response system of cucumber plants. However, under E[CO_2] conditions, SOD activity in severe drought treatment was higher than that in control and moderate drought treatment, which indicated that E[CO_2] could increase antioxidative capacity(Fig. 3). Cysteine proteinase inhibitor, which involved in the regulation of endogenous processes and in defense against pests and pathogens, was up-regulated by drought stresses. These results implied that cucumber seedlings could improve the ability of plants adapting to drought stress by regulating the expression of stress and defense response proteins.

Glutathione transferase is associated with oxidative stress and plays an important role in stressed plants (Berhane et al., 1994). Previous studies have shown that adversity induced the expression of *GST* (Marrs, 1996), and drought stress up-regulated glutathione transferase in wheat and *brassica napus* (Koh et al., 2015). In this study, in the condition of A[CO_2], moderate drought stress also up-regulated glutathione S-transferase F10. The contents of GSH and ASA and APX activity were also increased under moderate and severe drought stress, which alleviated oxidative damage of cucumber seedlings under drought stress (Figs. 3 and 4). Under moderate drought stress, E[CO_2] down-regulated NADPH-dependent aldo-keto reductase which function as detoxifiying enzyme by reducing a range of toxic aldehydes and ketones produced during stress, and significantly decreased MDA content under severe drought stress (Fig. 5). This indicated that toxic aldehydes or ketones induced by drought stress under E[CO_2] were less than that under A[CO_2].

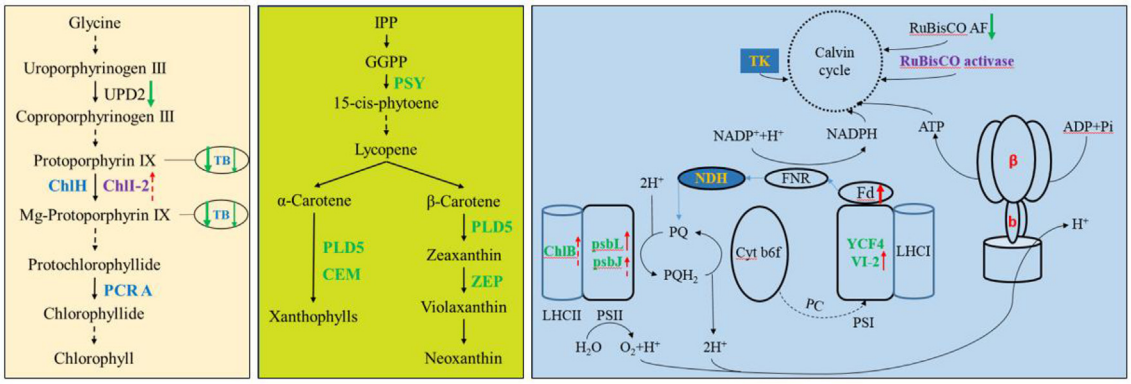

Fig. 9. Diagrammatic representation showing pathways of differentially expressed proteins involved in photosynthesis and pigment biosynthesis. Red letters represent proteins positive regulated by both moderate and severe drought stress; green letters represent proteins negative regulated by both moderate and severe drought stress; orange letters represent proteins positive regulated by severe drought stress; blue letters represent proteins negative regulated by moderate drought stress; purple letters represent proteins negative regulated by severe drought stress. Red arrows indicated up–regulation and green arrows indicated down–regulation by E[CO_2] under control (dashed lines), moderate drought stress (thin solid lines) and severe drought stress (thick solid lines). Abbreviations: UPD2: Uroporphyrinogen decarboxylase 2; TB: Tetrapyrrole-binding protein; ChlH: Magnesium-chelatase subunit ChlH; ChlI-2: Magnesium-chelatase subunit ChlI-2; PCRA: Protochlorophyllide reductase A; IPP: Isopentenyldiphosphate; GGPP: Geranylgeranyl diphosphatel; PSY: Phytoene synthase; PLD5: Protein LUTEIN DEFICIENT 5; CEM: Carotene epsilon-monooxygenase; ZEP: Zeaxanthin epoxidase; ChlB: Chlorophyll *a*/b binding protein; psbL: Photosystem II reaction center protein L; psbJ: Photosystem II reaction center protein J; Fd: Ferredoxin-2; YCF4: Photosystem I assembly protein Ycf4; VI-2: Photosystem I reaction center subunit VI-2; β: ATPsynthase subunit beta; b: ATPsynthase subunit b; TK: Transketolase; NDH: NAD(P)H-quinone oxidoreductase subunit 1; RuBisCO AF: RuBisCO accumulation factor 1.1.

4.3. Proteins involved in redox homeostasis

We found drought stresses up-regulated ferritin under the A[CO_2], which indicated that ferritin positively responded to drought stress. Moderate drought stress up-regulated Phospholipid hydroperoxide glutathione peroxidase (PHGPx) under the A[CO_2], indicating that cucumber seedlings can protect themselves from oxidative damage by increasing the expression of peroxidase under drought stress. In this study, less abundance of CBS domain-containing protein CBSX1 detected under severe drought stress and E[CO_2], but there was no significant increase in thioredoxin family protein, which indicated that the reduction of CBSX1 didn't reduce the expression of thioredoxin protein. Chloroplast CBSX1, ferredoxin, thioredoxins, adenosine-containing ligands, and target enzymes can regulate H_2O_2 levels and help to maintain cellular redox homeostasis and Calvin cycle activity by interacting with each other (Bertoni, 2011). It also showed that the regulation mechanism of E[CO_2] on the redox balance under drought stress was complicated and need to be further studied.

4.4. Proteins involved in metabolic pathways

Threonine dehydratase participates in the biosynthesis of isoleucine. It is the first speed-limiting enzyme in L-isoleucine biosynthesis pathway. Our results showed that severe drought stress and E[CO_2] up-regulated threonine dehydratase and promoted isoleucine biosynthesis under severe drought stress, and E[CO_2] significantly increased the content of proline compared with A[CO_2] (Fig. 5). These free amino acids induced by abiotic stress can act as osmotic regulators and play an important role in plant stress resistance. It also showed that E[CO_2] could improve drought resistance of cucumber by increasing the expression and content of osmolytes under drought stress.

Imidazole glycerol phosphate synthase his HF is an enzyme in the process of histidine metabolism. It participates in biosynthesis of L-histidine and abscisic acid. Probable N-acetyl-gamma-glutamyl-phosphate reductase participates in the biosynthesis of arginine, which has the highest efficiency for nitrogen storage. In this study, E[CO_2] down-regulated imidazole glycerol phosphate synthase his HF under moderate drought stress and N-acetyl-gamma-glutamyl-phosphate reductase under severe drought stress. Moreover, drought stresses down-regulated ferredoxin-nitrite reductase under E[CO_2] condition, which indicated that drought stress affected the reduction of nitrate and the absorption of nitrogen in the plant.

ATP-dependent zinc metalloprotease FTSH 6 is involved in the degradation of the light-harvesting complex of photosystem II (LHC II) during senescence or high light acclimation (Żelisko et al., 2005). Drought stresses increased its abundance under A[CO_2], but only moderate drought stress increased its abundance under E[CO_2] conditions, which indicated that E[CO_2] accelerating the degradation of the LHC II depends on degree of drought stress. Plant lipoxygenases may involve a number of diverse aspects of plant physiology including growth and development, pest resistance, and senescence or responses to wounding, and the synthesis of jasmonic acid caused by leaf wounding requires the participation of lipoxygenase (Bannenberg et al., 2008). In this study, drought stresses up-regulated lipoxygenase, showed that plants could improve the expression of lipoxygenase to alleviate the damage caused by drought stress, while E[CO_2] has no significant alleviating effect on drought stress.

5. Conclusion

Chloroplast proteins in response to [CO_2] and drought stress in cucumber seedlings were analyzed basically in this study. We herein provide an overview of the characteristic proteome related to pigment biosynthesis, photosynthesis, stress and defense response, redox homeostasis and metabolic pathways in the chloroplasts of cucumber leaves exposed to E[CO_2] and drought stresses. Combined with morphological and physiological data, this study revealed the mechanism underlying the increases in photosynthetic ability induced by E[CO_2] under drought conditions. E[CO_2] down-regulated pigment biosynthesis under drought conditions, which decreased the absorption of excess light energy, thus minimizing the effects of reactive oxygen species and photodamage induced by drought stress. E[CO_2] improved photosynthesis, antioxidant ability and osmotic adjustment ability, and relieved photodamage and accumulation of toxic substance under drought stress by regulating expression of chloroplast proteins such as those related to stress and defense response, redox homeostasis, metabolic pathways, which alleviate cucumber drought stress to some extents. However, screen and verification of the target protein still need to be further investigated.

Author contributions

Qingming Li and Dalong Zhang designed and supervised the project; Qingqing Cui, Yiman Li and Shuhao Li performed experiments; Qingqing Cui, Xinrui He and Binbin Liu analyzed data; Qingqing Cui and Qingming Li wrote the manuscript.

Acknowledgments

This work was supported by the National Natural Science Foundation of China (31471918, 31872154); the Shandong Key Research and Development Plan (2017CXGC0201); the Shandong Agricultural Major Application Technology Innovation (2016-36), and Science and Technology Innovation Team of Shandong Agricultural University-Protected Horticulture Advantageous Team (SYL2017YSTD07).

Appendix A. Supplementary data

Supplementary data to this article can be found online at https://doi.org/10.1016/j.plaphy.2019.08.025.

References

Ainsworth, E.A., Rogers, A., 2007. The response of photosynthesis and stomatal conductance to rising [CO_2]: mechanisms and environmental interactions. Plant Cell Environ. 30, 258–270. https://doi.org/10.1111/j.1365-3040.2007.01641.x.

Appenroth, K.J., Stöckel, J., Srivastava, A., Strasser, R.J., 2001. Multiple effects of chromate on the photosynthetic apparatus of *Spirodela polyrhiza* as probed by OJIP chlorophyll *a* fluorescence measurements. Environ. Pollut. 115, 49–64. https://doi.org/10.1016/S0269-7491(01)00091-4.

Baker, N.R., 1991. Possible role of photosystem II in environmental perturbations of photosynthesis. Physiol. Plant. 81, 563–570.

Bala, G., 2013. Digesting 400 ppm for global mean CO_2 concentration. Curr. Sci. 104, 1471–1472. http://eprints.iisc.ac.in/id/eprint/47066.

Bannenberg, G., Martínez, M., Hamberg, M., Castresana, C., 2008. Diversity of the enzymatic activity in the lipoxygenase gene family of *arabidopsis thaliana*. Lipids 44, 85–95. https://doi.org/10.1007/s11745-008-3245-7.

Bates, L.S., Waldren, R.P., Teare, I.D., 1973. Rapid determination of free proline for water-stress studies. Plant Soil 39, 205–207. https://doi.org/10.1007/BF00018060.

Benešová, M., Holá, D., Fischer, L., Jedelský, P.L., Hnilička, F., Wilhelmová, N., Rothová, O., Kočová, M., Procházková, D., Honnerová, J., Fridrichová, L., Hniličková, H., 2012. The physiology and proteomics of drought tolerance in maize: early stomatal closure as a cause of lower tolerance to short-term dehydration? PLoS One 7 (6), e38017. https://doi.org/10.1371/journal.pone.0038017.

Berhane, K., Widersten, M., Engström, A., Kozarich, J.W., Mannervik, B., 1994. Detoxication of base propenals and other alpha, beta-unsaturated aldehyde products of radical reactions and lipid peroxidation by human glutathione transferases. Proc. Natl. Acad. Sci. 91, 1480–1484. https://doi.org/10.1073/pnas.91.4.1480.

Bertoni, G., 2011. CBS domain proteins regulate redox homeostasis. The Plant Cell 23 3562-3562. https://doi.org/10.1105/tpc.111.231011.

Beyer, W.F., Fridovich, I., 1987. Assaying for superoxide dismutase activity: some large consequences of minor changes in conditions. Anal. Biochem. 161, 559–566. https://doi.org/10.1016/0003-2697(87)90489-1.

Carmo-Silva, A.E., Gore, M.A., Andrade-Sanchez, P., French, A.N., Hunsaker, D.J., Salvucci, M.E., 2012. Decreased CO_2 availability and inactivation of Rubisco limit photosynthesis in cotton plants under heat and drought stress in the field. Environ. Exp. Bot. 83, 1–11. https://www.sciencedirect.com/science/article/pii/S0098847212000883.

Canadell, J.G., Le, Q.C., Raupach, M.R., Field, C.B., Buitenhuis, E.T., Ciais, P., Conway, T.J., Gillett, N.P., Houghton, R.A., Marland, G., 2007. Contributions to accelerating atmospheric CO_2 growth from economic activity, carbon intensity, and efficiency of natural sinks. Proc. Natl. Acad. Sci. 104, 18866–18870. https://doi.org/10.1073/pnas.0702737104.

Chance, B., Maehly, A.C., 1955. [136] Assay of catalases and peroxidases. In: Methods in Enzymology, vol. 2. Academic Press, pp. 764–775. https://www.sciencedirect.com.

Chen, Y.J., Yu, J.J., Huang, B.R., 2015. Effects of elevated CO_2 concentration on water relations and photosynthetic responses to drought stress and recovery during re-watering in tall fescue. J. Am. Soc. Hortic. Sci. 140, 19–26. https://doi.org/10.21273/JASHS.140.1.19.

Cho, U.H., Park, J.O., 2000. Mercury-induced oxidative stress in tomato seedlings. Plant Sci. 156, 0–9. https://doi.org/10.1016/s0168-9452(00)00227-2.

Costa, M.C.D., Righetti, K., Nijveen, H., Yazdanpanah, F., Ligterink, W., Buitink, J., Hilhorst, H.W.M., 2015. A gene co-expression network predicts functional genes controlling the re-establishment of desiccation tolerance in germinated Arabidopsis thaliana seeds. Planta 242, 435–449. https://doi.org/10.1007/s00425-015-2283-7.

Crafts-Brandner, S.J., Salvucci, M.E., 2000. Rubisco activase constrains the photosynthetic potential of leaves at high temperature and CO_2. Proc. Natl. Acad. Sci. 97, 13430–13435. https://doi.org/10.1073/pnas.230451497.

Feng, G.Q., Li, Y., Cheng, Z.-M., 2014. Plant molecular and genomic responses to stresses in projected future CO_2 environment. Crit. Rev. Plant Sci. 33, 238–249. https://doi.org/10.1080/07352689.2014.870421.

Götz, S., García-Gómez, J.M., Terol, J., Williams, T.D., Nagaraj, S.H., Nueda, M.J., Robles, M., Talón, M., Dopazo, J., Conesa, A., 2008. High-through put functional annotation and data mining with the Blast2GO suite. Nucleic Acids Res. 36, 3420–3435. https://doi.org/10.1093/nar/gkn176.

Ghotbi-Ravandi, A.A., Shahbazi, M., Shariati, M., Mulo, P., 2014. Effects of mild and severe drought stress on photosynthetic efficiency in tolerant and susceptible barley (*Hordeum vulgare* L.) genotypes. J. Agron. Crop Sci. 200, 403–415. https://doi.org/10.1111/jac.12062.

Hao, X.Y., Li, P., Li, H.L., Zong, Y.Z., Zhang, B., Zhao, J.Z., Han, Y.H., 2016. Elevated CO_2 increased photosynthesis and yield without decreasing stomatal conductance in broomcorn millet. Photosynthetica 55, 176–183. https://doi.org/10.1007/s11099-016-0226-6.

Heath, R.L., Packer, L., 1968. Photoperoxidation in isolatedchloroplasts: I. Kinetics and stoichiometry of fatty acidperoxidation. Arch. Biochem. Biophys. 125, 189–198. https://doi.org/10.1016/0003-9861(68)90654-1.

Hsu, P.K., Takahashi, Y., Munemasa, S., Merilo, E., Laanemets, K., Waadt, R., Patera, D., Kollist, H., Schroeder, J.I., 2018. Abscisic acid-independent stomatal CO_2 signal transduction pathway and convergence of CO_2 and ABA signaling downstream of OST1 kinase. Proc. Natl. Acad. Sci. 115, E9971–E9980. https://doi.org/10.1073/pnas.1809204115.

Hyun, T.K., Graaff, E.V.D., Albacete, A., Eom, S.H., Großkinsky, D.K., Böhm, H., Janschek, U., Rim, Y., Ali, W.W., Kim, S.Y., 2013. The arabidopsis plat domain protein1 is critically involved in abiotic stress tolerance. PLoS One 9, e112946. https://doi.org/10.1371/journal.pone.0112946.

Irigoyen, J.J., Einerich, D.W., Sánchez-Díaz, M., 1992. Water stress induced changes in concentrations of proline and total soluble sugars in nodulated alfalfa (Medicago sativd) plants. Physiol. Plant. 84, 55–60. https://doi.org/10.1111/j.1399-3054.1992.tb08764.x.

Jaleel, C.A., Manivannan, P., Wahid, A., Farooq, M., Aljuburi, H.J., Somasundaram, R., Panneerselvam, R., 2009. Drought stress in plants: a review on morphological characteristics and pigments composition. Int. J. Agric. Biol. 11, 100–105. https://www.semanticscholar.org.

Kalaji, H.M., Jajoo, A., Oukarroum, A., Brestic, M., Zivcak, M., Samborska, I.A., Cetner, M.D., Łukasik, I., Goltsev, V., Ladle, R.J., 2016. Chlorophyll *a* fluorescence as a tool to monitor physiological status of plants under abiotic stress conditions. Acta Physiol. Plant. 38, 102. https://doi:10.1007/s11738-016-2113-y.

Kanehisa, M., Goto, S., Sato, Y., Furumichi, M., Tanabe, M., 2012. KEGG for integration and interpretation of large-scale molecular data sets. Nucleic Acids Res. 40, D109–D114. https://doi.org/10.1093/nar/gkr988.

Kirkham, M.B., 2011. Elevated Carbon Dioxide: Impacts on Soil and Plant Water Relations. CRC Press. https://doi.org/10.1201/b10812.

Koh, J., Chen, G., Yoo, M.J., Zhu, N., Dufresne, D., Erickson, J.E., Shao, H., Chen, S., 2015. Comparative proteomic analysis of brassica napus in response to drought stress. J. Proteome Res. 14, 3068–30815. https://doi.org/10.1021/pr501323d.

Kosmala, A., Perlikowski, D., Pawlowicz, I., Rapacz, M., 2012. Changes in the chloroplast proteome following water deficit and subsequent watering in a high- and a low-drought-tolerant genotype of Festuca arundinacea. J. Exp. Bot. 63, 6161–6172. https://doi.org/10.1093/jxb/ers265.

Li, M., Li, Y.M., Zhang, W.D., Li, S.H., Gao, Y., Ai, X.Z., Zhang, D.L., Liu, B.B., Li, Q.M., 2018. Metabolomics analysis reveals that elevated atmospheric CO_2 alleviates drought stress in cucumber seedling leaves. Anal. Biochem. 559, 71–85. https://doi.org/10.1016/j.ab.2018.08.020.

Li, Q.M., Liu, B.B., Wu, Y., Zou, Z.R., 2008. Interactive effects of drought stresses and elevated CO_2 concentration on photochemistry efficiency of cucumber seedlings. J. Integr. Plant Biol. 50, 1307–1317. https://doi.org/10.1111/j.1744-7909.2008.00686.x.

Li, Q.M., Liu, B.B., Zou, Z.R., 2011. Effects of doubled CO_2 concentration on photosynthetic characteristics of cucumber seedlings under drought stresses. China. Agric. Sci. 44, 963–971. https://doi.org/10.17660/ActaHortic.2012.936.11.

Ling, Q.H., Broad, W., Trösch, R., Töpel, M., Sert, T.D., Lymperopoulos, P., Baldwin, A., Jarvis, R.P., 2019. Ubiquitin-dependent chloroplast-associated protein degradation in plants. Science 363 eaav4467. https://www.ncbi.nlm.nih.gov/pubmed/30792274.

Liu, B.B., Li, M., Li, Q.M., Cui, Q.Q., Zhang, W.D., Ai, X.Z., Bi, H.G., 2017. Combined effects of elevated CO_2 concentration and drought stress on photosynthetic performance and leaf structure of cucumber (*Cucumis sativus* L.) seedlings. Photosynthetica 56, 942–952. https://doi.org/10.1007/s11099-017-0753-9.

Liu, G.T., Ma, L., Duan, W., Wang, B.C., Li, J.H., Xu, H.G., Wang, L.J., Yan, X.Q., Yan, B.F., Li, S.H., 2014. Differential proteomic analysis of grapevine leaves by iTRAQ reveals responses to heat stress and subsequent recovery. BMC Plant Biol. 110, 1–17. https://doi.org/10.1186/1471-2229-14-110.

Marrs, K.A., 1996. The function and regulation of glutathione-S-transferase in plants. Annu. Rev. Plant Biol. 47, 127–158. https://doi.org/10.1146/annurev.arplant.47.1.127.

Munné-Bosch, S., Alegre, L., 2000. Changes in carotenoids, tocopherols and diterpenes during drought and recovery, and the biological significance of chlorophyll loss in Rosmarinusofficinalis. plants. Planta 210, 925–931. http://www.jstor.org/stable/23385929.

Nakano, Y., Asada, K., 1981. Hydrogen Peroxide is scavenged by ascorbate-specific peroxidase in spinach chloroplasts. Plant Cell Physiol. 22, 867–880. https://doi.org/10.1093/oxfordjournals.pcp.a076232.

Nakayama, K., Okawa, K., Kakizaki, T., Inaba, T., 2008. Evaluation of the protective activities of a lateembryogenesis abundant (LEA) related protein, Cor15am, during

various stresses invitro. Biosci. Biotechnol. Biochem. 72, 1642–1645. https://doi.org/10.1271/bbb.80214.

Omran, R.G., 1980. Peroxide levels and the activities of catalase, peroxidase, and indoleacetic acid oxidase during and after chilling cucumber seedlings. Plant Physiol. 65, 407–408. https://doi.org/10.1104/pp.65.2.407.

Sandberg, A., Lindell, G., Källström, B.N., Branca, R.M., Danielsson, K.G., Dahlberg, M., Larson, B., Forshed, J., Lehtiö, J., 2012. Tumor proteomics by multivariate analysis on individual pathway data for characterization of vulvar cancer phenotypes. Mol. Cell. Proteom. 11, 1–14. https://doi.org/10.1074/mcp.M112.016998.

Strasser, B.J., 1997. Donor side capacity of photosystem II probed by chlorophyll a fluorescence transients. Photosynth. Res. 52, 147–155.

Wang, L.J., Huang, W.D., Li, J.Y., Liu, Y.F., Shi, Y.L., 2004. Peroxidation of membrane lipid and Ca^{2+} homeostasis in grape mesophyll cells during the process of cross-adaptation to temperature stresses. Plant Sci. 167, 71–77. https://doi.org/10.1016/j.plantsci.2004.02.028.

Wiśniewski, J.R., Zougman, A., Nagaraj, N., Mann, M., 2009. Universal sample preparation method for proteome analysis. Nat. Methods 6, 359–362. https://doi.org/10.1038/nmeth.1322.

Youssef, A., Laizet, Y.h., Block, M.A., Maréchal, E., Alcaraz, J.P., Larson, T.R., Pontier, D., Gaffé, J., Kuntz, M., 2010. Plant lipid-associated fibrillin proteins condition jasmonate production under photosynthetic stress. Plant J. 61, 436–445. https://doi.org/10.1111/j.1365-313X.2009.04067.x.

Żelisko, A., García-Lorenzo, M., Jackowski, G., Jansson, S., Funk, C., Lorimer, G.H., 2005. Atftsh6 is involved in the degradation of the light-harvesting complex ii during high-light acclimation and senescence. Proc. Natl. Acad. Sci. 102, 13699–13704. https://doi.org/10.1073/pnas.0503472102.

Zieske, L.R., 2006. A perspective on the use of iTRAQ™ reagent technology for protein complex and profiling studies. J. Exp. Bot. 57, 1501–1508. https://doi.org/10.1093/jxb/erj168.